A&A 387, 271–284 (2002)
DOI: 10.1051/0004-6361:20020381
© ESO 2002

Astronomy & Astrophysics

Radiative accelerations in stars: The effect of Zeeman splitting

G. Alecian[1] and M. J. Stift[2]

[1] DAEC/LUTH (Observatoire de Paris – CNRS), Observatoire de Meudon, 92195 Meudon Cedex, France
[2] Institut für Astronomie (IfA), Universität Wien, Türkenschanzstrasse 17, 1180 Wien, Austria
e-mail: stift@astro.univie.ac.at

Received 21 December 2001 / Accepted 8 March 2002

Abstract. The influence of Zeeman splitting on radiative accelerations of chemical elements in stellar atmospheres permeated by magnetic fields with strengths of up to a few Tesla has for the first time been investigated in detail taking into account magneto-optical effects and line blending. The work is based on the newly developed object-oriented and parallel code CARAT (which is presented in some detail), on extensive atomic data taken from the VALD database and on a 12 000 K, $\log g = 4.0$ Kurucz atmosphere with solar abundances. The calculations show that magnetically induced spectral line desaturation can lead to unexpectedly large amplifications of accelerations – relative to the zero-field case – in a number of atomic species. These amplifications are found to be strongly dependent both on field strength and on field orientation, reaching a pronounced maximum near the inclination of 60° between field vector and vertical with values sometimes in excess of 1.5 dex. Horizontal accelerations, a consequence of polarised radiative transfer, turn out to remain fairly small and will probably not have any important effect on the diffusion velocity vector. This first study on a large scale of how radiative accelerations are affected by Zeeman splitting is completed by a discussion of the importance of complete atomic line lists, in particular line lists with *correct* Landé factors; it must also be accepted that magneto-optical effects can by no means be neglected. Finally, it appears that the "canonical" picture of abundance inhomogeneities may have to be revised: instead of being tied to regions with predominantly vertical or horizontal magnetic fields, abundance patches could show up as contours about the curves tracing the field vector inclination of ≈60°.

Key words. diffusion – stars: abundances – stars: chemically peculiar – stars: magnetic fields – polarization

1. Introduction

The atmospheres of the chemically peculiar stars on the upper main sequence, the so-called CP stars, are often permeated by strong magnetic fields (some 10 mT to 3.5 T) and characterised by apparently large over-abundances of certain metals. At present, astrophysicists favour diffusion processes as the source of abundance anomalies, a scenario first elaborated by Michaud (1970). This idea has subsequently been followed up by a number of authors, enumerated in this introduction, to whom we refer the reader for a detailed discussion of the physics involved in radiative diffusion and the complex buildup of element stratification in stars (a review being outside the scope of this paper). Let us note that while considerable progress has been made during the last decade in the modelling of diffusion deep inside the stars – thanks to the availability of large new atomic and opacity databases for high degrees of ionisation – diffusion processes in stellar atmospheres have received very little attention. Now that observational evidence has accumulated that seems to establish beyond doubt the presence of variations in chemical abundances over the stellar surface (e.g. Strasser et al. 2001) and that gives strong hints at chemical stratification in the outer layers of CP stars (Bagnulo et al. 2001), there is renewed interest in the modelling of radiative diffusion in stellar atmospheres. A new approach to the problem of radiative diffusion in the outer layers of a star has been made possible by the tremendous increase in readily available computing power – harnessed by new parallel codes – combined with extensive atomic transition data well suited to detailed radiative transfer calculations and (polarised) spectral line synthesis, like the VALD database (Piskunov et al. 1995). Such new generation tools have been used for the modelling of diffusion in horizontal branch stars and in CP stars by Hui-Bon-Hoa et al. (2000, 2002).

One of the most challenging aspects of the study of CP stars is the modelling of abundance inhomogeneities in their magnetic atmospheres. As mentioned above, the presence of variations in chemical abundances over the stellar surface appears to be an established fact and Doppler Imaging results (e.g. Kuschnig et al. 1999) seem to suggest that these are somehow related to the strength and orientation of the magnetic field. Such conclusions should certainly be interpreted with the necessary caution but it is interesting to investigate whether there is

Send offprint requests to: G. Alecian,
e-mail: georges.alecian@obspm.fr

Article published by EDP Sciences and available at http://www.aanda.org or http://dx.doi.org/10.1051/0004-6361:20020381

a convincing physical explanation for these observations, and to produce observational predictions. Vauclair et al. (1979) have shown that – when the horizontal magnetic field component is strong enough to freeze the diffusion of silicon ions – silicon should be supported by the photons absorbed in its neutral state. This was confirmed in the quantitative study of Alecian & Vauclair (1981) who showed that silicon spots (or rings) are expected at places where magnetic lines are nearly parallel to the stellar surface. Gallium, in contrast, rather accumulates near places where the magnetic lines are nearly vertical, as found by Alecian & Artru (1987). Michaud et al. (1981) suggested that many other metals and rare earths behave in a similar way. A detailed study of aluminium is due to Hui-Bon-Hoa et al. (1996).

All the investigations enumerated so far have been made under the assumption that radiative accelerations are not affected by the magnetic field. Alecian & Vauclair (1981) for example have estimated that the role of Zeeman splitting could be neglected in the case of silicon lines and at field strengths less than about 1 Tesla. Zeeman splitting thus seemed to be of secondary importance and only the effect of the magnetic field on the diffusion coefficients (i.e. on the movements of the ions across magnetic lines, see Vauclair et al. 1979) were being considered.

To our knowledge, only Babel & Michaud (1991) (hereafter referred to as BM) have attempted to elucidate the behaviour of radiative accelerations in stellar atmospheres permeated by strong magnetic fields. Their analytical work however offers only limited insight since it is restricted to accelerations at the stellar surface in the case of a simple Zeeman triplet in a Milne-Eddington atmosphere, anomalous dispersion terms not being included. Unfortunately, also the accompanying study of the Sr II $\lambda\,4077$ line does not take into account magneto-optical effects – for the importance of the latter see Sect. 6.1. In addition, from the work of BM it is by no means clear how radiative accelerations change with Zeeman splitting in strongly blended spectra.

Keeping the incompleteness and the simplified physics of this investigation in mind, we have addressed many of the open questions, and we want to present in this paper an in-depth reassessment of the role of Zeeman splitting on the radiative accelerations of the different chemical elements. Our results are based on Kurucz model atmospheres (Kurucz 1993), on new large atomic databases, in particular VALD (Piskunov et al. 1995), and on a new LTE diffusion code CARAT (Code pour les Accélérations Radiatives dans les ATmosphères) that incorporates the best affordable input physics and that can execute on massively parallel multiprocessor machines.

2. Polarised radiative transfer

The equation for radiative transfer of polarised light can be written:

$$\frac{\mathrm{d}}{\mathrm{d}z}\,\boldsymbol{I} = -\boldsymbol{K}\;\boldsymbol{I} + \boldsymbol{j} = -\boldsymbol{K}\,(\boldsymbol{I}-\boldsymbol{S}) \tag{1}$$

where z is the vertical position in the stellar atmosphere (positive outwards), $\boldsymbol{K}$ the absorption matrix (line plus continuum), $\boldsymbol{j}$ the total emission vector, and $\boldsymbol{S} = \boldsymbol{K}^{-1}\,\boldsymbol{j}$ the source function. $\boldsymbol{I}$ is the Stokes vector $\{I,Q,U,V\}^\dagger$ (transpose) where I represents the intensity, Q and U characterise the linear polarisation, and V the circular polarisation (for a gentle introduction to polarised radiative transfer see Rees 1987). Stokes vector and absorption matrix are functions of frequency ν.

$$\boldsymbol{S} \;=\; \{B_\nu(T),0,0,0\}^\dagger, \tag{2}$$

$$\boldsymbol{K} \;=\; \kappa_\mathrm{c}\,\mathbf{1} + \kappa_\mathrm{o}\,\boldsymbol{\Phi}. \tag{3}$$

Here κ_c stands for the continuum opacity, $B_\nu(T)$ for the Planck function, κ_o denotes the line centre opacity for zero damping and zero magnetic field, $\mathbf{1}$ is the unit 4×4 matrix. The line absorption matrix

$$\boldsymbol{\Phi} = \begin{pmatrix} \eta_I & \eta_Q & \eta_U & \eta_V \\ \eta_Q & \eta_I & \rho_V & -\rho_U \\ \eta_U & -\rho_V & \eta_I & \rho_Q \\ \eta_V & \rho_U & -\rho_Q & \eta_I \end{pmatrix}$$

depends on strength, direction γ and azimuth χ of the magnetic field. The line absorption terms become

$$\eta_I \;=\; \tfrac{1}{4}\,(2\,\eta_\mathrm{p}\,\sin^2\!\gamma + (\eta_\mathrm{r}+\eta_\mathrm{b})(1+\cos^2\gamma)) \tag{4}$$

$$\eta_Q \;=\; \tfrac{1}{4}\,(2\,\eta_\mathrm{p} - (\eta_\mathrm{r}+\eta_\mathrm{b}))\,\sin^2\gamma\,\cos 2\chi \tag{5}$$

$$\eta_U \;=\; \tfrac{1}{4}\,(2\,\eta_\mathrm{p} - (\eta_\mathrm{r}+\eta_\mathrm{b}))\,\sin^2\gamma\,\sin 2\chi \tag{6}$$

$$\eta_V \;=\; \tfrac{1}{2}\,(\eta_\mathrm{r}-\eta_\mathrm{b})\,\cos\gamma \tag{7}$$

and the Faraday terms

$$\rho_Q \;=\; \tfrac{1}{4}\,(2\,\rho_\mathrm{p} - (\rho_\mathrm{r}+\rho_\mathrm{b}))\,\sin^2\gamma\,\cos 2\chi \tag{8}$$

$$\rho_U \;=\; \tfrac{1}{4}\,(2\,\rho_\mathrm{p} - (\rho_\mathrm{r}+\rho_\mathrm{b}))\,\sin^2\gamma\,\sin 2\chi \tag{9}$$

$$\rho_V \;=\; \tfrac{1}{2}\,(\rho_\mathrm{r}-\rho_\mathrm{b})\,\cos\gamma \tag{10}$$

where the line absorption profiles for the π and for the blue or red shifted σ components – the shifts are directly proportional to the magnetic field strength – are denoted by $\eta_{\mathrm{p,\,b,\,r}}$ respectively, and where the $\rho_{\mathrm{p,\,b,\,r}}$ are the corresponding anomalous dispersion profiles.

3. Radiative accelerations in a magnetic atmosphere

The total radiative acceleration of an ion $A(+i)$, in a given atmospheric layer, is obtained by determining the total amount of momentum gained per second by absorption of photons. To compute this total amount of momentum, one generally integrates over frequency the photoabsorption cross-sections of all atomic transitions of $A(+i)$ multiplied by the local radiation flux. Actually, the situation is complicated by the fact that acceleration due to photoionisation (see for instance Alecian 1994; Gonzalez et al. 1995) must be redistributed to ion $A(i+1)$ and must take into account the momentum taken away by the ejected electron (Massacrier 1996). But since at present we are interested solely in studying the effect of Zeeman splitting of lines, we hereafter restrict ourselves to the momentum

acquired through bound-bound transitions, i.e. the radiative accelerations due to absorption in spectral lines.

The radiative acceleration due to lines in the non-magnetic case can be calculated considering (in the integral over frequencies) only the net photon flux, and using the following well-known scalar expression:

$$g_i^{\rm rad} = \sum_{k,m>k} \frac{n_{ik}}{n_i\, A\, m_{\rm p}\, c} \int_\nu^\infty \sigma_{km}\, \Phi(\nu, n_i)\, {\rm d}\nu. \qquad (11)$$

In the case of a magnetic field, the spatial symmetry around the z-axis is lost and the acceleration vector is now given by

$$\boldsymbol{g}_i^{\rm rad} = \sum_{k,m>k} \frac{n_{ik}}{n_i\, A\, m_{\rm p}\, c} \int_\Omega \int_\nu (\boldsymbol{e}\cdot\boldsymbol{I})\, \boldsymbol{\Omega}\, {\rm d}\Omega\, {\rm d}\nu \qquad (12)$$

where

- n_i is the total number density (m^{-3}) of ions A^{+i}, n_{ik} the number density of ions in initial lower level k,
- $A\, m_{\rm p}$ is the mass (kg) of the ion,
- σ_{km} is the absorption cross-section (m^2) for the transition $k \rightarrow m$,
- Φ is the net energy flux ($\mathrm{W}\cdot\mathrm{m}^{-2}\cdot\mathrm{Hz}^{-1}$),
- $(\boldsymbol{e}\cdot\boldsymbol{I})$ denotes the inner product of the vector $\boldsymbol{e} = \kappa_{\rm o}\{\eta_I, \eta_Q, \eta_U, \eta_V\}$ with the Stokes vector $\boldsymbol{I}$.

It has to be emphasised that the angles γ and χ in the vector $\boldsymbol{e}$ do *not* depend on the direction of the magnetic field vector relative to the observer but relative to the direction of the pencil of radiation. Let us also note that inclusion of the full Stokes vector can lead to an acceleration vector that is no longer purely vertical.

4. Radiative accelerations: Computational requirements

In order to calculate realistic radiative accelerations of chemical elements in stellar atmospheres permeated by strong magnetic fields, it is necessary to treat line blending and Zeeman splitting in full detail, and to solve the polarised radiative transfer equation with an accurate formal solver, e.g. the Zeeman-Feautrier solver of Auer et al. (1977). Line blending can be quite heavy at short wavelengths in most CP stars, so any approximate treatment is bound to fail. In a similar vein, the polarised radiative transfer in the outer layers of these stars cannot adequately be described by the diffusion approximation.

Calculation of the frequency integrals in the formulae (11) and (12) given in the previous section is best done employing the trapezoidal rule. In fact, the integrand – essentially the product of flux times line opacity – can vary significantly over wavelength intervals of the order of a couple of mÅ. Such behaviour is demonstrated in Fig. 1 – keep in mind that the figure displays the *logarithm* of the integrand – and precludes the use of higher-order integration schemes. Good accuracy can only be achieved with fairly high wavelength resolution; it turns out that the spectral range 900−10 000 Å has to be sampled at least

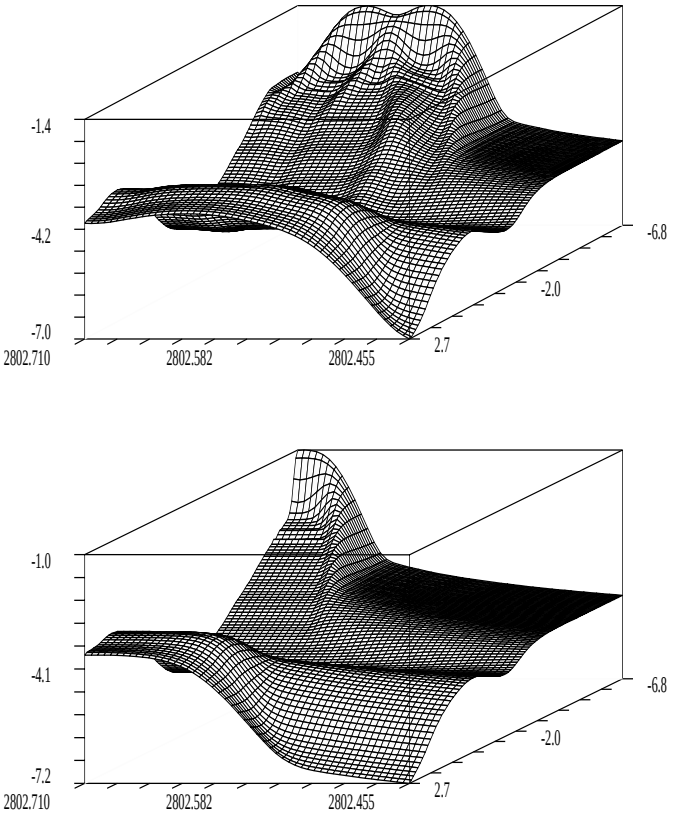

Fig. 1. Mg II λ 2802: run with wavelength and with logarithmic standard optical depth $\log\tau_{5000}$ of $\log(\boldsymbol{e}\cdot\boldsymbol{I})$ – as defined in Sects. 2 and 3 and in $\mathrm{W}\cdot\mathrm{Hz}^{-1}\cdot\mathrm{sterad}^{-1}$. For the sake of clarity, only the blue half of the line is displayed. **Bottom:** zero magnetic field, **Top:** horizontal field of 2 T. The pencil of light in the direction $\mu = 0.183$ sees a nearly transverse magnetic field vector (81°). Stark broadening has been calculated according to Gonzalez et al. (1995) but with a coefficient of 6.0×10^{-6} (Artru, private communication).

every 10 mÅ, but it is advisable to go down to a 5 mÅ step size.

Thus all of the more than 2×10^6 Zeeman components contributing to the opacity have to be sampled at the 1.8×10^6 quadrature points in wavelength. Subsequently, the wavelength integrals have to be integrated over all spatial directions, which in the general case of a magnetic field vector arbitrarily inclined towards the vertical implies a 2-D integration with typically 24 quadrature points. Only in the case of a longitudinal field can the problem be reduced to a 1-D integration (4 points should be sufficient).

Solving the polarised transfer equation 4.4×10^7 times (with about 100 points in optical depth) in addition to sampling the opacity of 2×10^6 Zeeman components at 1.8×10^6 wavelength points is very time-consuming and outside the reach of even the fastest single-processor machines, if acceptable turnaround times are to be attained. As an illustration of the computational requirements, a single run with a 24 point 2D-integration requires some 64 hours mono-processor time on an Sgi Origin 3800 computer equipped with the R14000 chip. This corresponds to about 97 hours on a 1 GHz AMD or Intel processor according to our benchmarks (secondary cache size

plays some role). Thus we have to employ (massively) parallel computing in order to calculate realistic radiative accelerations in magnetic atmospheres, based on the best input physics available.

5. CARAT: Code pour les Accélérations Radiatives dans les ATmosphères

There was no code that would meet the physical, numerical and computational requirements outlined above, so a new code had to be developed. CARAT is based on the object-oriented and parallel polarised spectral line synthesis code COSSAM (Codice per la sintesi spettrale nelle atmosfere magnetiche) a description of which is provided by Stift (2000) and by Wade et al. (2001). Written entirely in *Ada95*, the only standardised (ISO/IEC 8652:1995) *object-oriented* language with *concurrent constructs*, CARAT and COSSAM are based on truly reusable software components which incorporate software engineering concepts such as abstract data types, encapsulation and information hiding, generics, inheritance and programming by extension (see Stift 1996, 1998a for more details on Ada95 in (astro)physics). About 68% of the software components used in CARAT, representing more than 4000 lines of code (4 kLOCs) have been taken verbatim from COSSAM. Thanks to its *thread-parallel* approach, Ada95 does not require the use of Message Passing Interfaces – as in Fortran – in order to exploit the "embarrassingly parallel" nature of the spectral line synthesis problem. We refer to Stift (1998b) for a detailed discussion of concurrency and lightweight synchronisation with Ada95 in this astrophysical context.

5.1. Numerics

For the solution of the polarised radiative transfer problem we have chosen the Zeeman Feautrier method of Auer et al. (1977) instead of the more popular and somewhat faster DELO method (Rees et al. 1989). The reason for this lies in the legendary stability of the Feautrier method, in the fact that it is second order accurate – in contrast to DELO's first order accuracy, see Stift (1999) – and that it automatically recovers the diffusion approximation at great depths (Mihalas 1978). The latter is particularly important for radiative accelerations which depend on the net Stokes flux. Magneto-optical terms are normally included in the formal solution but there is a runtime option to suppress them for test purposes.

Tables of continuous opacities $\kappa_{\rm c}\,(\lambda, \tau_{5000})$ as a function of wavelength and the given standard optical depth grid are extracted from the Atlas 9 (Kurucz 1993) output files. CARAT interpolates in this table at every 5 mÅ step. The total line opacity $\kappa_{\rm l}\,(\lambda, \tau_{5000})$ is determined by full opacity sampling of the σ_-, the σ_+, and π components separately.

Spatial integration of the frequency integrated product of Stokes flux times radiative cross section is carried out in 2 steps. The frequency integral is first integrated over all azimuthal angles around the z-axis, employing the trapezoidal rule; as in the case of frequency integration, the ill-behaved nature of the integrand precludes the use of higher-order integration schemes. Subsequently, a Gaussian quadrature is carried out over $\mu = \cos\theta$, usually based on 4 quadrature points. Extensive tests have shown that a total of 4 quadrature points in μ and of 6 in azimuth, i.e. a total of 24 points, are sufficient for fairly accurate radiative accelerations, i.e. substantially better than 1%.

5.2. The underlying physics of CARAT

Some of the input physics in CARAT can be traced back to "Analyse 65", the ALGOL 60 code by Baschek et al. (1966) and to its evolved FORTRAN translation ADRS 3 (Chmielewski 1979). The atomic transitions are taken from the VALD database (Piskunov et al. 1995). The atomic partition functions are normally calculated with the Kurucz (1993) routine rewritten in Ada95 but one can also choose the partition functions by Traving et al. (1966), Irwin (1981) or Cowley (1998). CARAT works under the assumption of LTE in a plane-parallel atmosphere; in the Saha equation the lowering of the ionisation potential as a function of temperature and electron density is taken into account. Generally, radiation damping and van der Waals broadening constants are taken from VALD; classical radiation damping and Unsöld van der Waals broadening respectively are assumed if these constants are not provided by VALD. Concerning Stark broadening there are 2 options: either Stark broadening is taken form VALD and set to zero whenever not available, or Stark broadening is calculated for all transitions using the formula discussed by Gonzalez et al. (1995) but with a coefficient of 6.0×10^{-6} (Artru, private communication) instead of the original 8.0×10^{-6}. It is clear that not only is there the necessity of including state-of-the-art accurate hydrogen line opacities, but that reliable hydrogen line blanketed continuous radiative fluxes can only be obtained by a correct treatment of the Balmer discontinuity. We have chosen to interpolate in the tables of hydrogen profiles by Stehlé & Hutcheon (1999) and to treat the higher Balmer series members according to the recipe given in Hubeny et al. (1994), based on the occupation probability formalism discussed in Hummer & Mihalas (1988), Däppen et al. (1987) and Seaton (1990). Metallic line profiles are calculated by the rational approximation to the Voigt and Faraday functions given in Landolt-Börnstein (1982).

6. Zeeman patterns and VALD

For many, but by no means for all lines, VALD lists Landé factors in addition to the J-values of the respective lower and upper energy levels, which makes it possible to calculate Zeeman splittings outside LS coupling. Relative component strengths are derived with the help of the formulae given in Sobelman (1979). Complications in splittings and relative intensities due to the partial Paschen-Back effect are not taken into account.

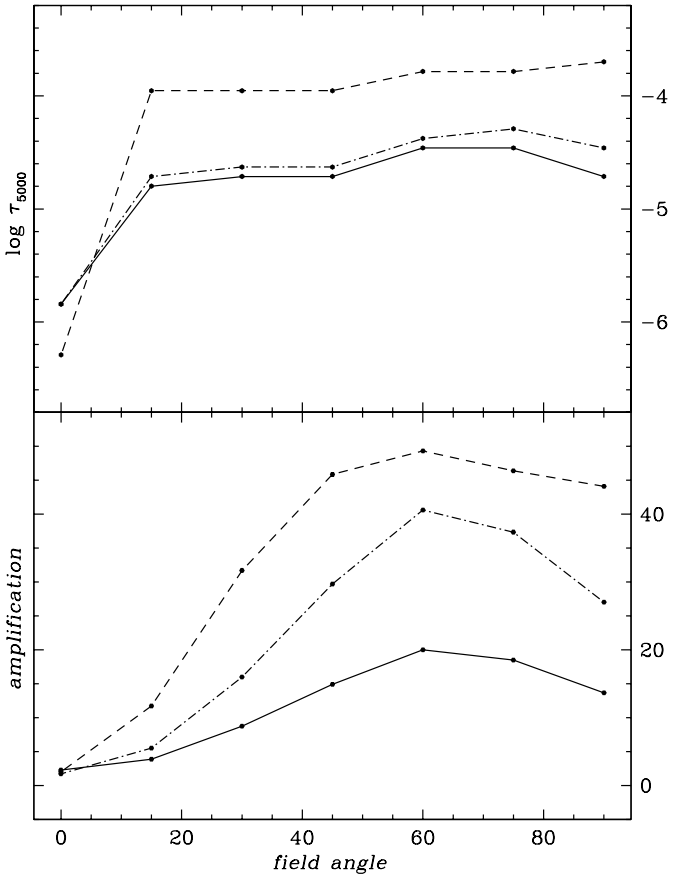

Fig. 2. Radiative accelerations due to the Mg II lines at λ 2795.5 and λ2802.7 (no blending with lines of other elements considered) in a 2 T magnetic field, relative to the zero field case. **Bottom:** Maximum magnetic amplification of acceleration (over all optical depths) as a function of the angle between the vertical and the magnetic field vector (in degrees). Results are shown for the correct sextuplet and quadruplet (solid line), the same without magneto-optical effects included (short dash), and for classical triplets (dot – short dash). **Top:** The corresponding location in the atmosphere where maximum magnetic amplification occurs.

A problem arises with those lines for which VALD does not provide Landé factors. Whereas in the case of Fe I through Fe III for which Zeeman data are complete to 99.996% one could simply assume classical Zeeman triplets without affecting the final results, there are a number of elements – among them Mg, Al, Si and Zn – where VALD does not list any Landé factors at all, not even those of the strongest lines. It has been known for a long time (see Babcock 1949) that magnetic intensification due to desaturation caused by Zeeman-splitting varies considerably between simple triplets and complex anomalous Zeeman patterns. As a consequence, radiative accelerations calculated with classical Zeeman triplets only may be seriously in error, as is evident from Fig. 2 where we find overestimates by a striking 100%. As a consequence, one must get Landé factors from various listings of atomic energy levels (at least for the resonance lines), a most tedious but essential step in the quest for accurate radiative accelerations, which cannot however be extended to tens of thousands of lines. The solution for the latter case consists in the use of the spectroscopic term classifications provided by VALD for the determination of Landé factors under the assumption of LS-coupling. This is far less demanding, but since it is well known that LS-coupling does not hold universally – see Stift (1977) for a few illustrations – the resulting Zeeman patterns of individual lines might be seriously in error. Still, there is the well-founded hope that statistically the result will not go too far astray, especially when the Landé factors of the strongest lines are taken from accurate energy level tables.

6.1. Magneto-optical effects

It has already been pointed out by Landolfi et al. (1989) and reemphasised by Wade (2000) that the inclusion of magneto-optical effects is critical for the correct interpretation of Stokes profiles in CP stars. In the Mg II λ 2795.5 and λ2802.7 resonance lines, at field strengths of up to 2 T, the σ-components overlap with the π-components. Cyclical coupling in the polarised radiative transfer equation of Q, U and V as a result of anomalous dispersion, and coupling of Stokes I with the Stokes parameters Q, U and V due to absorption should play an important role in these extremely strong lines. We expect accelerations to be considerably affected.

In order to investigate this further, we have carried out detailed calculations for the Mg II resonance lines in a 2 T magnetic field under 3 different assumptions, viz.

1. taking the sextuplet and quadruplet patterns (i.e. the correct Zeeman splitting);
2. the same with magneto-optical effects omitted;
3. assuming both lines to be classical triplets.

Figure 2 displays the respective radiative accelerations relative to the zero field case at various inclinations between the magnetic field vector and the vertical. We note that the accelerations as a function of angle invariably exhibit a maximum near 60° – regardless of the assumption – but that these maxima differ by large amounts. At 60° the magnetic amplification factor based on the correct Zeeman patterns takes a value near 20; under the simplifying assumption of the lines being Zeeman triplets this value doubles. The exclusion of magneto-optical effects introduces even more severe errors, artificially increasing the amplification factor to a value of 50. Let us also point out another systematic effect which results from the omission of the Faraday terms. Figure 2 (top) reveals that maximum amplification, enhanced by a substantial 0.4 dex over the correct value, occurs in significantly deeper layers.

There is nothing strange in the fact that the inclusion of anomalous dispersion terms leads to a reduction in acceleration. In fact, the decrease in flux and concomitant increase in equivalent width due to magneto-optical effects is well established (see Landolfi et al. 1989). Multiplication of the cross section – which remains unchanged – with a reduced flux quite naturally leads to a drop in acceleration. Only the extent to which this can happen in very strong

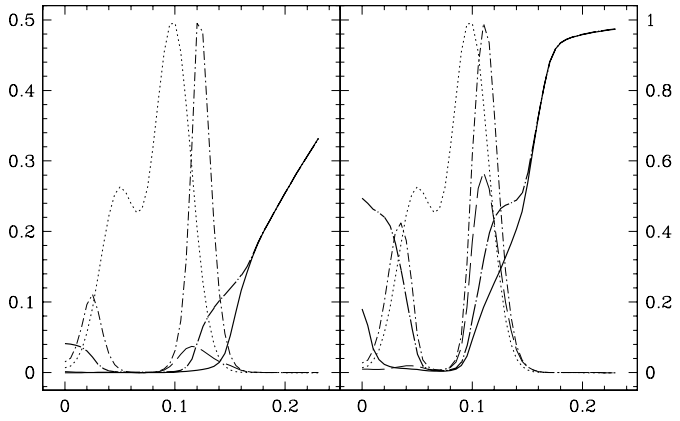

Fig. 3. Mg II $\lambda\,2802$: run with $\Delta\lambda$ (reckoned from the line centre) at standard optical depth $\log\tau_{5000} = 3.445 \times 10^{-3}$ of the normalised flux in Stokes I, with (full line) and without (dot – long dash) anomalous dispersion terms considered. In addition, the plot shows the shape of η_I (dotted line) and the relative sizes of the vertical accelerations, with (long dash) and without (dot – short dash) magneto-optical effects. The angle between the magnetic field vector and the ray in the direction $\mu = 0.53$ is about 77°, the magnetic field strength 2 T. The left panel pertains to the true strength of the line, the right panel to the line with 100 times lower oscillator strength.

lines, with a ratio of line centre opacity to continuous opacity of 10^5 and more as in the case of the Mg II resonance lines, may appear somewhat surprising, but can easily be explained. Taking the solution for a Milne-Eddington atmosphere (see e.g. Rees 1987), we have

$$I = B_0 + \mu B_1[(1+\eta_I)((1+\eta_I)^2 + \boldsymbol{\rho}\cdot\boldsymbol{\rho})]/\Delta \tag{13}$$

where

$$\Delta = (1+\eta_I)^2[(1+\eta_I)^2 - \boldsymbol{\eta}\cdot\boldsymbol{\eta} + \boldsymbol{\rho}\cdot\boldsymbol{\rho}] - (\boldsymbol{\eta}\cdot\boldsymbol{\rho})^2 \tag{14}$$

$$\boldsymbol{\rho} = \{\rho_Q, \rho_U, \rho_V\} \tag{15}$$

$$\boldsymbol{\eta} = \{\eta_Q, \eta_U, \eta_V\}\cdot \tag{16}$$

In the $\lambda\,2802$ Mg II resonance line a detailed analysis reveals that the spectacular decrease in acceleration due to magneto-optical effects stems from the fact that both in the outer parts of this quadruplet line and near the centre, the term $(1+\eta_I)^2(\boldsymbol{\rho}\cdot\boldsymbol{\rho}) - (\boldsymbol{\eta}\cdot\boldsymbol{\rho})^2$ dominates the term $(1+\eta_I)^4 - (1+\eta_I)^2(\boldsymbol{\eta}\cdot\boldsymbol{\eta})$ by 4 to 6 orders of magnitude. The dominating term brings the residual flux obtained without anomalous dispersion in the (component-free) line centre down to almost the low levels encountered between the π- and the σ-components. Similarly, it leads to a substantial drop in flux in the outer wings of the σ-components. The stronger the line, the more important this effect becomes, as can be seen in Fig. 3. Strong lines behave in an exceptionally interesting way, discussed to some length in Sect. 8; the full details of this behaviour remain yet to be documented.

Our calculations convincingly demonstrate that it is of paramount importance, especially in such strong lines, to employ the correct Zeeman pattern and to include magneto-optical effects in the formal solution of the polarised radiative transfer equation. The latter can be easily done at virtually no extra cost, employing the Zeeman-Feautrier solver, but the former constitutes at present a major problem. Indeed, atomic databases such as VALD do not yet provide the necessary Zeeman data for all elements and we would like to encourage the VALD people to direct efforts in this direction.

7. Detailed computations

Thanks to extensive systematic computations of radiative accelerations in stellar atmospheres permeated by strong magnetic fields, which we have carried out with CARAT, we are now able to estimate the effect of Zeeman splitting on all ions for which line data are available in VALD. Hydrogen and helium excepted, where radiative accelerations are not relevant in CP star atmospheres, we have data for 329 ions (ionisation degrees smaller than 5) of the 90 elements from Li to U. We have chosen a Kurucz Atlas9 model with $T_{\rm eff} = 12\,000$ K and $\log g = 4.0$ which, although it does not represent a realistic CP star atmosphere, is sufficiently well suited for our present investigation which centres on the *difference* between accelerations derived from Zeeman split spectra and accelerations due to lines unaffected by magnetic fields. The temperature range encountered in this model determines the wavelength interval for which significant photon flux is available: we have carried out our calculations from 900 Å to 10 000 Å, including all those lines from VALD for which the central opacities at any depth point reach at least 10^{-3} of the continuum opacity at this location. In the present calculations this leads to the inclusion of 140 087 spectral lines, split into 739 099 σ_-, 739 099 σ_+ and 764 366 π components respectively. No VALD tools have been employed.

In order to study the radiative diffusion of elements, the b-b radiative accelerations of all ions of a given element must be combined with the accelerations due to photoionisation (not computed here). Generally this is done through some weighted mean of the $g_i^{\rm rad}$ and involves the relative ion populations, the collision rates with protons, and the ionisation and recombination rates for each ion (Montmerle & Michaud 1976; Alecian & Vauclair 1983; Gonzalez et al. 1995). Theses calculations are outside the scope of this work since we are only interested in the role of the Zeeman splitting. For our purposes we shall therefore use the following simple approximation to the total radiative acceleration of an element

$$g^{\rm rad} = \frac{\Sigma n_i g_i^{\rm rad}}{\Sigma n_i} \tag{17}$$

where n_i stands for the population and $g_i^{\rm rad}$ for the radiative acceleration in ionisation stage i. The sum extends over all ionisation stages provided in the Kurucz partition function routine.

Our simple formula has, among others, the advantage of reducing the amount of numerical results to analyse. A mere 90 accelerations have to be considered instead

of 329. Moreover, this approximation is helpful for the purpose of having a first estimate of how an element behaves: when $g^{\rm rad}$ is larger than gravity, the element is pushed up by the radiation field. The magnetic field enters our results solely through Zeeman splitting, and that is what we are presently interested in. However, for realistic diffusion studies, a future version of CARAT will of course have to include effects like redistribution of momentum among ions of the same element, photoionisation, and the dependence of the diffusion coefficients on the magnetic field.

7.1. The zero field case

Figure 4 shows $\log g_{\rm rad}$ (in cgs units) for all elements in the case of zero magnetic field and solar chemical composition. Note that elements for which $g_{\rm rad}$ is always smaller than $10\,{\rm cm\,s^{-2}}$ (e.g. Li), or for which no line has been extracted from VALD (see above), do not appear in Fig. 4. In general, abundant metals like CNO and the iron peak elements display rather small accelerations (less than gravity) because of strong saturation of their lines. Let us emphasise that we have considered homogeneous solar abundances and that these accelerations can change considerably if diffusion proceeds for some time and stratification of elements appears.

For the reasons outlined above we have limited ourselves to the use of Eq. (13), so unfortunately no comparison is possible between the zero-field total radiative accelerations presented in Fig. 4, based on CARAT, and those obtained in LTE by Hui-Bon-Hoa et al. (2002). We believe that the accelerations of ions calculated with Eq. (11) are as accurate as those of Hui-Bon-Hoa et al. (2002) because of the state-of-the-art physics, numerics and radiative transfer employed in COSSAM, on which CARAT is based (see Wade et al. 2001). A partial comparison has been made with results from an older code used by Hui-Bon-Hoa et al. (1996), which has yielded satisfactory agreement in the case of the Al resonance line.

It must be noted that the accuracy of the accelerations depends on the quality and the completeness of the atomic data. We deem it highly probable that for several elements, (among them the rare earths and the heaviest elements), not all b-b transitions which contribute significantly to the respective accelerations are listed in VALD or in any other publicly accessible atomic database. Still, in the present work this presents no real problem since we are interested in *differential* effects only. The zero-field accelerations shown in Fig. 4 are to be considered reference values – sufficiently accurate up to the iron peak elements – against which we compare the magnetic results to be presented below. We want to warn that no direct quantitative conclusions about chemical peculiarities in CP stars can be drawn from our results.

7.2. The effect of Zeeman splitting

The effect of Zeeman splitting on the radiative accelerations has been calculated for 3 different field strengths, viz. 1, 2, and 4 Tesla, and a number of inclinations between the magnetic field vector and the surface normal. As it turns out, not only Mg II reaches maximum acceleration near an inclination of 60° but this behaviour is characteristic of all ionisation stages of all elements. These findings are at variance with the results for a Milne-Eddington atmosphere derived by BM who found maximum acceleration at 90° for all 7 Zeeman patterns investigated. However, a possible relation to the 55° found by BM for radiation propagating along the z-axis cannot be excluded. Given the physical simplifications underlying the Milne-Eddington solution, we do not deem it useful to further discuss theses discrepancies.

In Fig. 5 we plot the logarithmic amplification (at 60°) $\epsilon = \log g^{\rm rad}({\rm magnetic}) - \log g^{\rm rad}({\rm nonmagnetic})$ for all elements as a function of standard optical depth. For the sake of clarity, only those elements are displayed where the increase in $g^{\rm rad}$ exceeds 30% ($|\epsilon| > 0.11394$ dex) at any depth point in the atmosphere. The respective curves are labeled with the name of the corresponding element and the labels are placed at the location of the maximum.

Among the elements, Mg and Ca exhibit a truly spectacular increase of $g^{\rm rad}$ with magnetic field strength, with amplification factors at 4 T in excess of 40 and 10 respectively. At a more moderate 1 T field strength, the effect of magnetic splitting is less dramatic, but the amplification for Ca, Fe, Ni, and Zn still attains values of 2 and more in layers with $-4 < \log \tau_{5000} < 0$. In many cases, such as Mg, the amplification ϵ depends almost entirely on a few strong resonance lines. Keeping in mind that Zeeman splitting goes with the square of the wavelength, it is not surprising that the favourable combination of wavelength and extreme strength of the Mg II resonance lines near 2800 Å leads to a particularly effective desaturation and ensuing increase in radiative acceleration.

After all, it is not overly suprising to find amplification factors of certain elements that exceed by more than 1 order of magnitude those determined by BM. In fact, the behaviour with respect to magneto-optical effects of the Mg II λ2802 resonance line, displayed in Fig. 3, lets one expect similar large changes in flux due to Zeeman splitting. Accelerations in very strong lines subject to Zeeman splitting will be discussed later in the next section.

In the light of these results, we once more have to emphasise how important it is to employ accurate atomic data, not only oscillator strengths, but also Landé factors, especially for the resonance lines. Radiative accelerations of the lighter elements in a stellar atmosphere permeated by strong magnetic fields will therefore be seriously in error if they are based on VALD data that are not supplemented by Landé factors as pointed out above in Sect. 6.

Note that our calculations for Si, which yield an increase in acceleration of less than 30% for fields below 2 T, are in satisfactory accord with the predictions by Alecian & Vauclair (1981), based on a qualitative estimate of Zeeman desaturation.

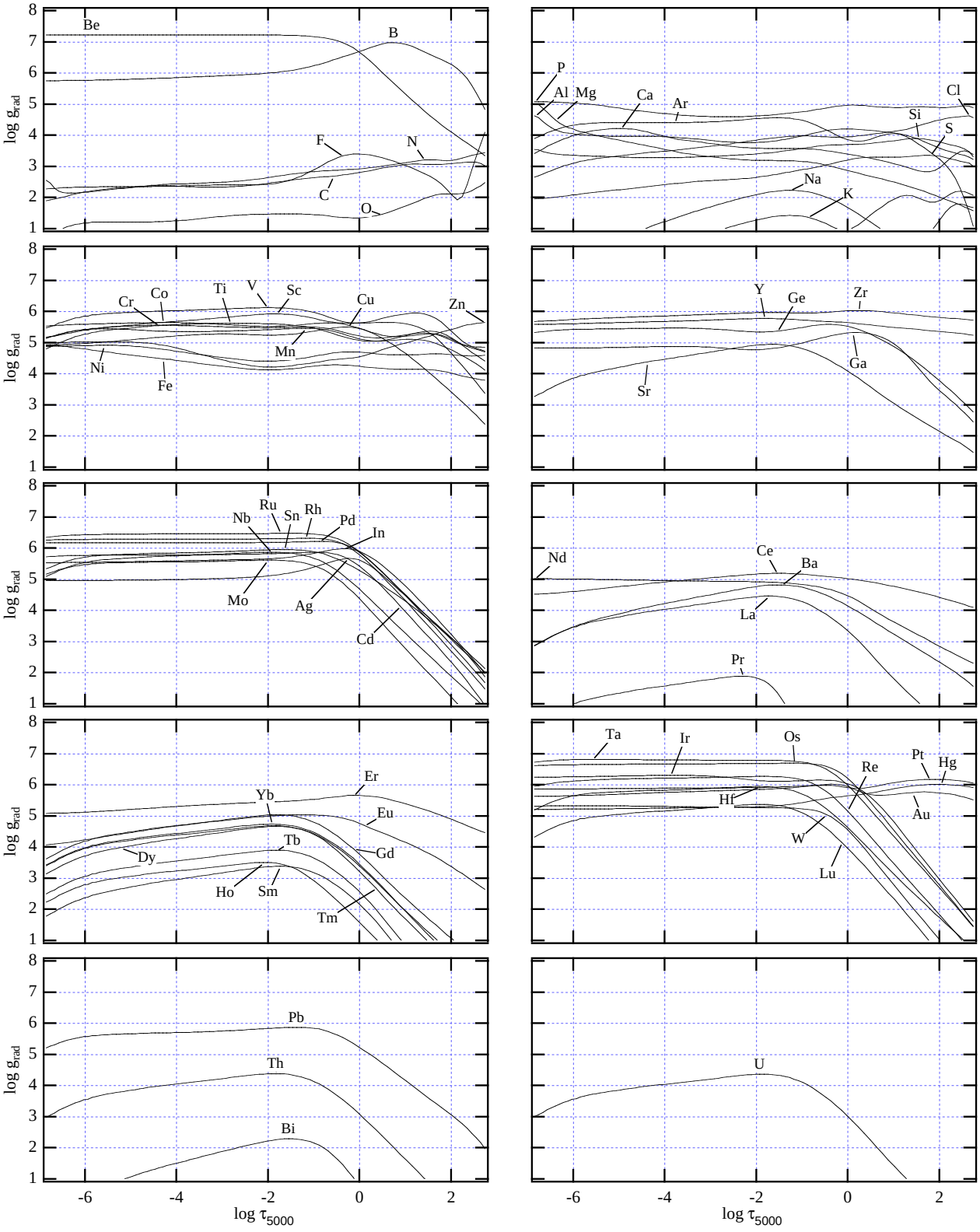

Fig. 4. Zero magnetic field radiative accelerations of the chemical elements in a Kurucz ATLAS9 $T_{\rm eff} = 12\,000$ K, $\log g = 4.0$ model atmosphere with solar composition. Accelerations are in cgs units to conform with Kurucz. Logarithmic accelerations are plotted vs. logarithmic standard optical depth at 5000 Å. The 10 panels are sorted by atomic numbers.

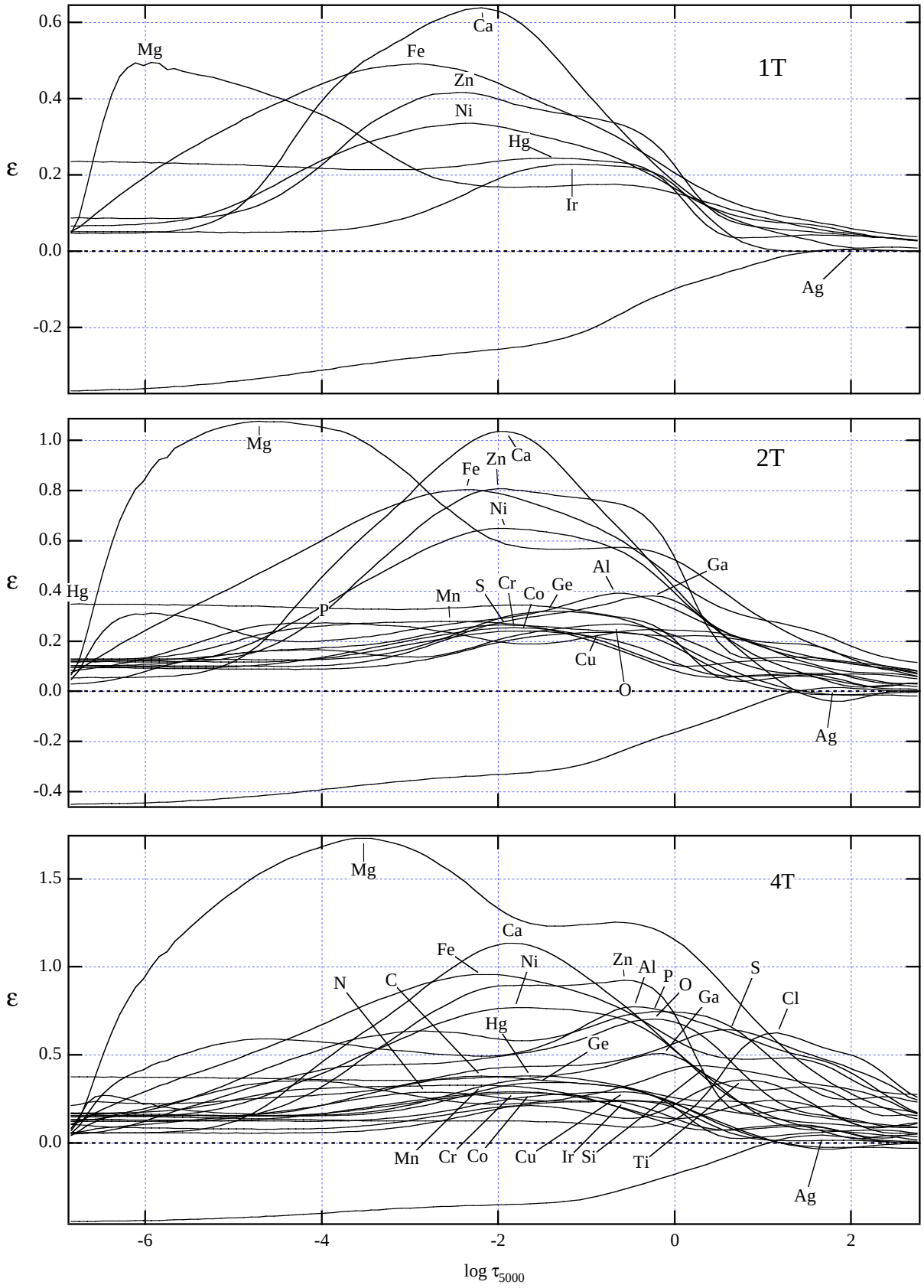

Fig. 5. Amplification of the radiative accelerations of the chemical elements due to Zeeman splitting as a function of optical depth and of magnetic field strength. Logarithmic amplifications $\epsilon = \log g^{\rm rad}(\text{magnetic}) - \log g^{\rm rad}(\text{nonmagnetic})$, defined relative to the accelerations shown in Fig. 4, are displayed for field strengths of 1, 2, and 4 T at a constant 60° angle between magnetic field vector and vertical. Curves are plotted only when $|\epsilon| > 0.11394$ dex at any depth point.

7.2.1. Ag, a special case

The acceleration of a species is essentially given by the product of photon flux times the cross section of the lines of this species. In principle, accelerations could either decrease, increase or remain unchanged with magnetic field strength, depending on the extent to which the drop in flux is counter-balanced by a different distribution with frequency of cross sections. It thus appears surprising that among the 90 elements for which we have calculated radiative accelerations, we have encountered only one case, viz. Ag, where Zeeman splitting leads to a significant decrease in $g^{\rm rad}$.

Our findings are compatible with the view that for most elements, a few strong lines rather than the ensemble of all lines dominate the total acceleration. If instead the latter resulted from almost equal contributions of a multitude of lines of comparable strength, more or less evenly distributed over the whole spectrum, one would, on statistical grounds, expect more cases of acceleration decreasing with magnetic splitting.

In the case of Ag, strong lines are absent and blending appears to be serious. Detailed calculations including just lines of Ag and hydrogen reveal the usual increase in acceleration with field strength in accord with our interpretation.

7.3. Horizontal accelerations

We have pointed out previously that the inclusion of the full Stokes parameters can lead to an acceleration vector that is no longer purely vertical. The deviation from the vertical turns out to be rather modest in those layers where the vertical acceleration $g_z^{\rm rad}$ exceeds gravity, just a few degrees. Interestingly, the horizontal acceleration $g_z^{\rm rad}$ does not always have the same sign for all optical depth points.

We do not think at present that horizontal accelerations will have any important effect on the diffusion velocity vector. Actually, even in the case of strictly vertical acceleration, the diffusion velocity vector can have a horizontal component of the same order of magnitude as the vertical component, because charged particles tend to follow the inclined field lines (see Alecian & Vauclair 1981; Michaud et al. 1981). As a note of caution we would like to add that, even in this case, observable effects of horizontal diffusion are most unlikely since the geometric scales involved are far larger than those of vertical diffusion (Alecian 1986).

8. Polarised radiative transfer and radiative acceleration in strong lines

The logarithmic amplifications of Mg and Ca revealed in Fig. 5 reach a surprising $\epsilon > 1$ at a field strength of 2 T. There follow Fe, Zn and Ni where $0.65 \leq \epsilon \leq 0.80$, but for the remaining 85 elements even a meagre $\epsilon = 0.4$ is rarely attained. What are the physical reasons for these huge differences in amplification among the various elements? Can we be sure that these results are not merely artefacts of our numerical scheme?

The Mg resonance lines at $\lambda\,2795.5$ and $\lambda\,2802.7$ are among the strongest 10 of the 140 087 lines used in our calculations. When Zeeman splitting of these lines causes desaturation and ensuing change in the outgoing flux, even a minor change can lead to a significant increase in acceleration because $\Delta\boldsymbol{I}$ has to be multiplied by the huge value of $\boldsymbol{e}$ (up to a few 10^7).

Egidio Landi Degl'Innocenti (private communication) has pointed out to us the difficulties that can arise when dealing with very strong lines. We reproduce his arguments almost verbatim. Consider the force which is exerted on an element of matter that is close to the surface and suppose that this force is due only to the radiation that is propagating upwards. Suppose also that the magnetic field is vertical. The η_I and η_V become

$$\eta_I = (\eta_{\rm r} + \eta_{\rm b})/2 \tag{18}$$
$$\eta_V = (\eta_{\rm r} - \eta_{\rm b})/2. \tag{19}$$

The intensity can be decomposed in right and left hand circular polarisation

$$I = I_{\rm r} + I_{\rm l} \tag{20}$$
$$V = I_{\rm r} - I_{\rm l}. \tag{21}$$

The acceleration is proportional to

$$\eta_I I = (\eta_{\rm r} I_{\rm r} + \eta_{\rm b} I_{\rm l} + \eta_{\rm r} I_{\rm l} + \eta_{\rm b} I_{\rm r})/2 \tag{22}$$
$$\eta_V V = (\eta_{\rm r} I_{\rm r} + \eta_{\rm b} I_{\rm l} - \eta_{\rm r} I_{\rm l} - \eta_{\rm b} I_{\rm r})/2 \tag{23}$$

and summing up one finds the obvious result

$$\eta_I I + \eta_V V = \eta_{\rm r} I_{\rm r} + \eta_{\rm b} I_{\rm l}. \tag{24}$$

But in extremely strong lines, the terms that cancel out analytically in the sum are very much larger than the other two that contribute to the sum. We have

$$\eta_{\rm r} I_{\rm l} >> \eta_{\rm r} I_{\rm r} \tag{25}$$
$$\eta_{\rm b} I_{\rm r} >> \eta_{\rm b} I_{\rm l} \tag{26}$$

because the component $\eta_{\rm r}$ overlaps with the continuum in left hand circular polarisation, whereas it overlaps with the line profile in right hand circular polarisation.

In practice this means that, since we cannot take advantage of this analytical cancellation, accelerations in strong lines are just tiny differences between the very large numbers $\eta_I I, \eta_Q Q, \eta_U U$ and $\eta_V V$. Which implies among others that we have to carry out all our calculations in double precision, but also that any simple analysis and visualisation – based on just the Stokes I parameter – of the acceleration as a function of frequency and depth becomes impossible.

In the course of the verification of the correct functioning of the CARAT code, we were confronted with seemingly strange behaviour of the flux in very strong lines. Taking the well-known solution for a Milne-Eddington

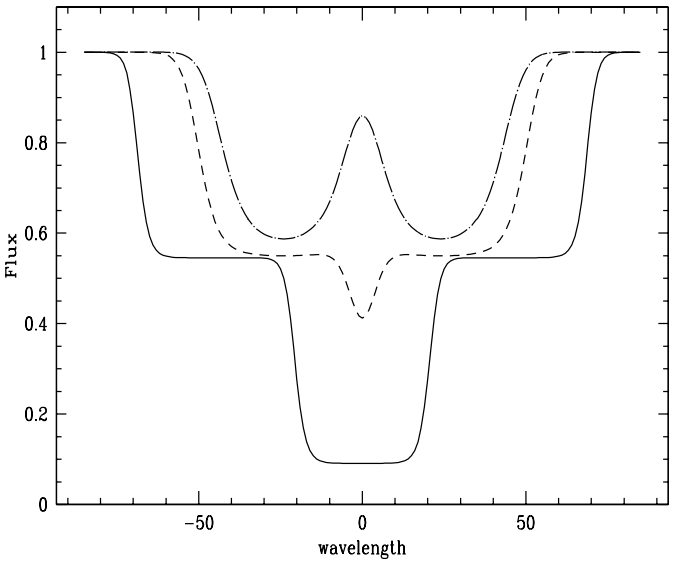

Fig. 6. Stokes I profile of a Zeeman triplet in a Milne-Eddington atmosphere with a source function $B = B_0(1+10\,\tau)$. The line profiles are assumed to be Gaussians with 12 mÅ half width, the splitting is 24 mÅ. Ratios of central line opacities over continuum opacity are $10^6, 10^2$ and 10, respectively (full, dashed, dot-dashed lines).

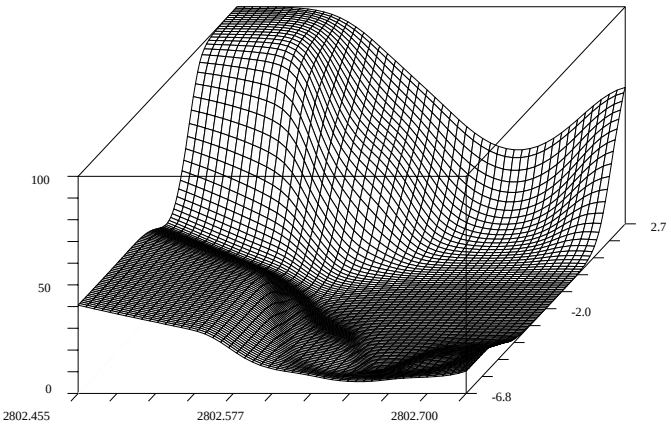

Fig. 7. Mg II $\lambda\,2802$: run with wavelength and with logarithmic standard optical depth $\log\tau_{5000}$ of the flux in Stokes I, normalised to the continuum value at each depth. For the sake of clarity, only the blue half of the line is displayed. The magnetic field of strength 2 T is horizontal, the pencil of light in the direction $\mu = 0.960$ sees a nearly transverse magnetic field vector (74°).

atmosphere (Rees 1987), a classical Zeeman triplet and a longitudinal magnetic field, one derives the following expression for the emerging Stokes I

$$I = B_0 + \mu\, B_1 \frac{(1 + \eta_\mathrm{r}/2 + \eta_\mathrm{b}/2)}{(1 + \eta_\mathrm{r} + \eta_\mathrm{b} + \eta_\mathrm{r}\,\eta_\mathrm{b})}. \qquad (27)$$

Under these conditions, the intensity of a moderately strong line reaches its minimum value of $I = B_0 + \mu\, B_1/2$ at the respective positions of the σ-components, with an increase in flux at the centre of the line (dot-dashed line in Fig. 6). This familiar picture changes for a stronger line (dashed) where the flux at the centre decreases below the value encountered at the respective positions of the σ-components, and finally in a line of comparable strength to that of the Mg II resonance lines, we have $I = B_0$ at the line centre where $\eta_\mathrm{r} = \eta_\mathrm{b} \gg 1$ (full line). Somewhat counter-intuitively one now finds a deep central depression; proceeding outwards, the flux increases until it reaches a plateau with $I = B_0 + \mu\, B_1/2$ at the position of the σ-component before attaining the continuum value much further out.

That such behaviour is not restricted to Milne-Eddington atmospheres is illustrated in Fig. 7. The plot of flux in Stokes I vs. wavelength and depth is characterised by what we may call, in analogy to oceanography, an "abyssal plain"; again, plateaus can be recognised, starting just outside the positions of the σ-components.

8.1. Where in the line does amplification occur?

It is possible to derive an analytical expression for the acceleration in the case of a transversal magnetic field and a Milne-Eddington atmosphere,

$$g_\mathrm{rad} \propto \frac{B_0}{2}(\eta_\mathrm{p} + \eta_\mathrm{rb}) + \frac{\mu\, B_1}{2}\left(\frac{\eta_\mathrm{p}}{1+\eta_\mathrm{p}} + \frac{\eta_\mathrm{rb}}{1+\eta_\mathrm{rb}}\right) \qquad (28)$$

with $\eta_\mathrm{rb} = (\eta_\mathrm{r} + \eta_\mathrm{b})/2$. A Zeeman split line will experience considerably less acceleration in its centre than the unsplit line, but this is slightly over-compensated by the acceleration in the σ-components. The numerical solution shows that this is indeed the case in the outermost layers, but reveals that throughout the rest of the atmosphere there is no such sharp drop in acceleration near the line centre (Fig. 8). In view of the results displayed in Fig. 6, it comes as no surprise that the "ridges" in the amplification surface which are due to the σ-components drift towards the wings of the line, whereas those due to the π-components drift towards the centre, both disappearing at the location of the "abyssal plain" where there is no amplification. Only in the deepest layers where the line opacity decreases, do we find again the "ridges" with a much reduced amplitude.

8.2. Mg versus Ca and Si

A systematic search yields 10 lines with a ratio of central line opacity over continuum opacity (at any depth point in the atmosphere) $\kappa_\mathrm{o}/\kappa_\mathrm{c} > 10^7$. There are another 40 lines with $\kappa_\mathrm{o}/\kappa_\mathrm{c} > 10^6$, 171 lines with $\kappa_\mathrm{o}/\kappa_\mathrm{c} > 10^5$, and 584 lines with $\kappa_\mathrm{o}/\kappa_\mathrm{c} > 10^4$, representing the elements C, N, O, Mg, Al, Si, P, S, Ca, Cr, Mn, Fe, Ni, Cu, Zn.

It may seem disturbing that, although the very strongest line in our list is that of Si II $\lambda\,1194.5$, the acceleration of Si exhibits only modest amplifications. One has however to keep in mind that the Si II $\lambda\,1194.5$ line is subject to 5 times smaller Zeeman splitting and to 34 times higher radiation damping than the Mg resonance lines. In order to quantify the effect of damping, we have

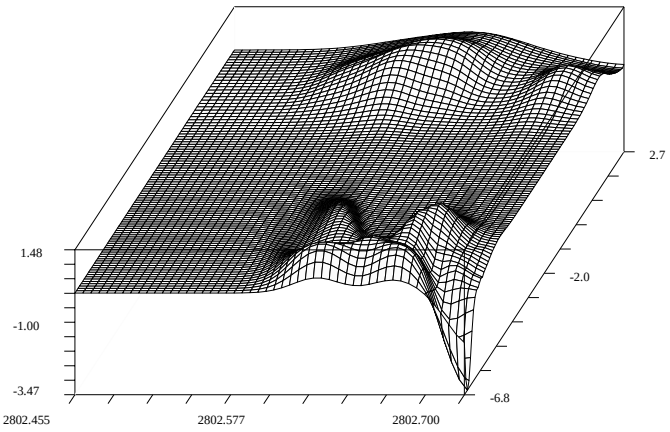

Fig. 8. Mg II λ 2802: run with wavelength and with logarithmic standard optical depth $\log \tau_{5000}$ of the acceleration per Hertz in a 2 T horizontal field, relative to the zero field case. For the sake of clarity, only the blue half of the line is displayed. The acceleration has been multiplied – for each layer – by a factor proportional to the index of this layer, in order to visually enhance the "ridges" at the bottom of the atmosphere which otherwise would be hard to detect. The pencil of light is in the same direction as in Fig. 7.

artificially multiplied the radiation damping constant of the Mg II λ 2802.7 line by a factor of 34. Figure 9 demonstrates that the zero-field acceleration now becomes larger – the full line corresponds to the original line data, the dash-dotted line to the artificially high damping – but that amplification drops to dramatically low values.

A similar experiment can be carried out in view of explaining the behaviour of Ca. The Ca H and K lines are more than 2 orders of magnitude weaker than the strongest Mg and Si lines, but Ca is still subject to very large amplifications. Artificially lowering the strength of the Mg II λ 2802.7 line by a factor of 100, we find that amplification remains large (dotted line in Fig. 9); it is also hardly affected when the abundance is decreased by 1 dex (dashed line).

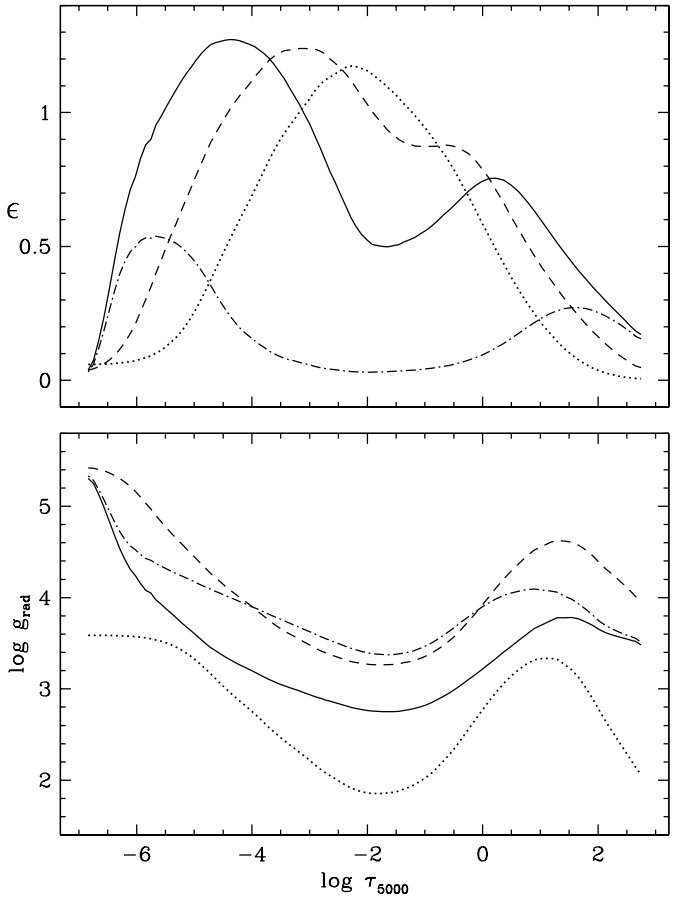

Fig. 9. Mg II λ 2802: amplification ϵ (top panel) in a 2 T magnetic field inclined by 60° with respect to the vertical and zero-field acceleration (bottom panel). The full lines give the results for the correct atomic data, the dash-dotted lines correspond to radiation damping artifically increased by a factor of 34. A decrease in abundance by 1 dex leads to the dashed line, a decrease in oscillator strength by a factor of 100 to the dotted line.

9. Conclusions

Thanks to the development of the new object-oriented and thread-parallel diffusion code CARAT – written entirely in Ada95 – it has now become possible to calculate reasonably accurate radiative acceleration vectors in stellar atmospheres permeated by strong magnetic fields, running the code on powerful symmetric multiprocessing machines. Taking the atomic line data from VALD (Piskunov et al. 1995), hydrogen line opacities from the tables of Stehlé & Hutcheon (1999) and treating the higher Balmer series members according to the recipe given in Hubeny et al. (1994), CARAT deals with line blending and Zeeman splitting in full detail, employing the Zeeman Fautrier polarised formal solver which recovers the diffusion approximation at great depths.

Our extensive and detailed computations convincingly demonstrate that the effect of Zeeman splitting on radiative accelerations can be much larger than what had been estimated previously. Whereas BM claim that even in the most favourable case (complex Zeeman pattern and horizontal field), the amplification factor is limited to a value of 2.3, we have found amplification factors ranging from about 8 to 50 at a field strength of 4 T in elements like Mg, Ca, Fe, Zn. Even for magnetic fields of 1 T strength, the amplification factor can reach a value of 4. We therefore conclude that in general, Zeeman splitting cannot be neglected in diffusion studies of magnetic stars, that it may well be the main cause of strong abundance inhomogeneities, and that any conclusions based on unreliable magnetic geometries and on calculations including just a few lines must be considered premature.

Our results are also in striking contradiction with the weak angular dependence of the vertical accelerations and with the small (10%) difference between respective accelerations for horizontal and vertical magnetic field found by BM. In the upper panel of Fig. 10 the maximum acceleration at a field strength of 2 T can be seen to exceed the minimum value (for vertical field) by factors of

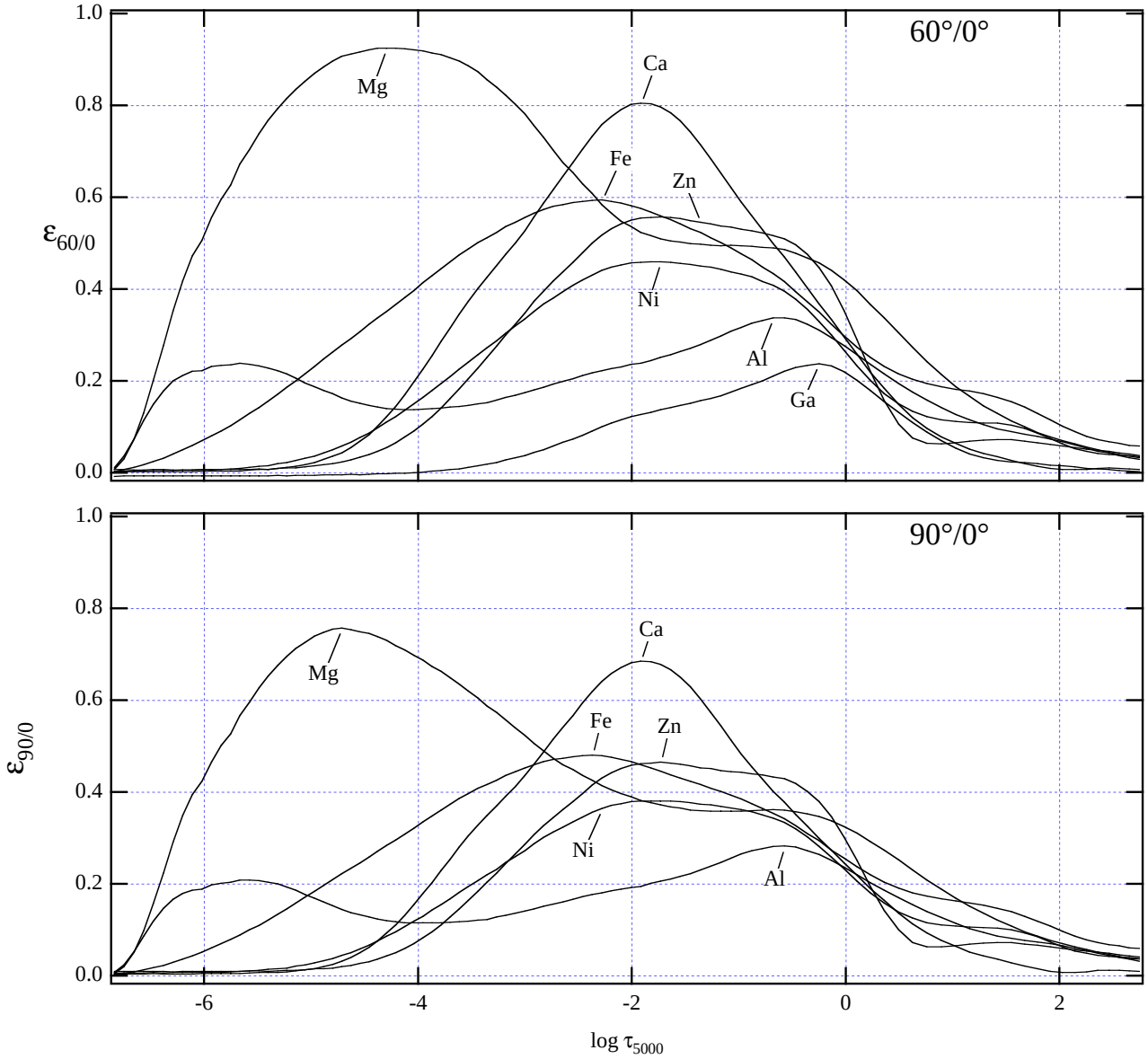

Fig. 10. Amplification ratio $\epsilon_{60/0} = \log g^{\rm rad}(60°) - \log g^{\rm rad}(0°)$ (upper panel), and $\epsilon_{90/0} = \log g^{\rm rad}(90°) - \log g^{\rm rad}(0°)$ (lower panel), computed for a 2 T magnetic field strength. We have plotted only curves with $\epsilon_{60/0} > 0.11394$ dex at any depth in the upper panel, with $\epsilon_{60/90} > 0.04139$ dex in the lower panel.

up to 10. Differences of 60% and more between $g^{\rm rad}(90°)$ and $g^{\rm rad}(0°)$ are encountered for Mg, Ca, Fe, Zn, Ni, Al, and Ga as shown in the bottom panel.

The large amplification factors ϵ and the strong sensitivity of amplification to the field angle suggests to us that the correlation between the magnetic geometry and the abundance inhomogeneities on the surface of magnetic CP stars may differ significantly from the "canonical" picture. The latter supposes that patches of over- or under-abundances are tied to those regions where the magnetic field lines are preferentially vertical or horizontal. It would now seem that abundance enhancements can occur at other places than the magnetic poles or the magnetic equator; for certain elements they could conceivably show up as contours about the curves tracing the field vector inclination of about 60° to the vertical. In the context of a multipole surface field structure (see Bagnulo & Landolfi 1999) abundance maps would become very complicated indeed.

The study of radiative diffusion in the atmospheres of CP stars permeated by strong magnetic fields has finally reached the next stage. Instead of having to restrict ourselves to a few lines, neglecting Zeeman splitting and employing approximate solutions to the radiative transfer equation, we can at last rely on (and afford) reasonably complete atomic transition data – including Landé factors – together with the correct treatment of magnetic blends and the use of an accurate polarised radiative transfer. CARAT, an object-oriented and parallel new code, meets these requirements and after the incorporation of further physical processes such as photoionisation and momentum redistribution among ions we expect it to be an efficient

tool in the exploration of diffusion processes in magnetic CP stars and ultimately in the modelling of the buildup of abundance inhomogeneities.

Acknowledgements. MJS acknowledges support by the *Austrian Science Fund (FWF)*, project P12101-AST "Solar and Stellar Magnetic Polarisation" and a Visiting Professorship at the Observatoire de Paris-Meudon (DAEC) and Université Paris 7 (DAEC/LUTH). The calculations have been carried out on the Sgi Origin 2000 and Origin 3800 of the CINES in Montpellier. We are heavily indebted to Egidio Landi Degl'Innocenti for masterly (and patient) explanations of the workings of polarisation.

References

Alecian, G. 1986, in Upper Main Sequence Stars With Anomalous Abundances, IAU Colloq. 90, ed. C. R. Cowley, M. M. Dworetsky, & C. Megessier (D. Reidel, Dordrecht), 381
Alecian, G. 1994, A&A, 289, 885
Alecian, G., & Artru, M.-C. 1987, A&A, 186, 223
Alecian, G., & LeBlanc, F. 2000, MNRAS, 319, 677
Alecian, G., & Vauclair, S. 1981, A&A, 101, 16
Alecian, G., & Vauclair, S. 1983, Fund. Cosmic Phys., 8, 369
Auer, L. H., Heasley, J. N., & House, L. L. 1977, ApJ, 216, 531
Babcock, H. W. 1949, ApJ, 110, 126
Babel, J., & Michaud, G. 1991, A&A, 241, 493 (BM)
Bagnulo, S., & Landolfi, M. 1999, A&A, 346, 158
Bagnulo, S., Wade, G. A., Donati, J.-F., et al. 2001, A&A, 369, 889
Baschek, B., Holweger, H., & Traving, G. 1966, Abh. Hamburger Sternwarte, Band VIII, 26
Chmielewski, Y. 1979, Publ. Obs. de Genève, Série B, Fasc. 7
Cowley, C. R. 1998, `ftp://astro.lsa.umich.edu/pub/get/cowley/partition/bolpfn.f`
Däppen, W., Anderson, L., & Mihalas, D. 1987, ApJ, 319, 195
Gonzalez, J.-F., LeBlanc, F., Artru, M.-C., & Michaud, G. 1995, A&A, 297, 223
Hubeny, I., Hummer, D. G., & Lanz, T. 1994, A&A, 282, 151
Hui-Bon-Hoa, A., Alecian, G., & Artru, M.-C. 1996, A&A, 313, 624
Hui-Bon-Hoa, A., LeBlanc, F., & Hauschildt, P. H. 2000, ApJ, 535, L43
Hui-Bon-Hoa, A., LeBlanc, F., Hauschildt, P. H., & Baron, E. 2002, A&A, 381, 197
Hummer, D. G., & Mihalas, D. 1988, ApJ, 331, 794
Irwin, A. W. 1981, ApJS, 45, 621
Kurucz, R. 1993, CDROM Model Distribution, Smithsonian Astrophys. Obs.
Kuschnig, R., Ryabchikova, T. A., Piskunov, N. E., Weiss, W. W., & Gelbmann, M. J. 1999, A&A, 348, 924
Landolfi, M., Landi degl'Innocenti, M., & Landi degl'Innocenti, E. 1989, A&A, 216, 113
Landolt-Börnstein 1982, Zahlenwerte und Funktionen aus Naturwissenschaften und Technik, Neue Serie, Gruppe VI: Astronomie, Astrophysik und Weltraumforschung, Band 2, Teilband b, ed. K. Schaifers, & H. H. Voigt, 107
Massacrier, G. 1996, A&A, 309, 979
Michaud, G. 1970, ApJ, 160, 641
Michaud, G., Megessier, C., & Charland, Y. 1981, A&A, 103, 244
Mihalas, D. 1978, Stellar atmospheres, 2nd edition (W.H. Freeman, San Francisco)
Montmerle, T., & Michaud, G. 1970, ApJS, 31, 489
Piskunov, N. E., Kupka, F., Ryabchikova, T. A., Weiss, W. W., & Jeffery, C. S. 1995, A&AS, 112, 525
Rees, D. E. 1987, in Numerical Radiative Transfer, ed. W. Kalkofen (Cambridge Univ. Press, Cambridge), 213
Rees, D. E., Murphy, G. A., & Durrant, C. J. 1989, ApJ, 339, 1093
Seaton, M. J. 1990, J. Phys. B, 23, 3255
Sobelman, I. I. 1979, Atomic Spectra and Radiative Transitions (Springer, Berlin), 193
Stehlé, C., & Hutcheon, R. 1999, A&AS, 140, 93
Stift, M. J. 1977, Ap&SS, 46, 465
Stift, M. J. 1996, in Model Atmospheres and Spectrum Synthesis, ed. S. J. Adelman, F. Kupka, & W. W. Weiss, ASP Conf. Ser., 108, 217
Stift, M. J. 1998a, Comp. Phys., 12, 150
Stift, M. J. 1998b, in Reliable Software Technologies – Ada Europe '98, ed. L. Asplund, Lect. Notes Comp. Sci., 1411, 128
Stift, M. J. 1999, in Solar Polarization, ed. K. N. Nagendra, & J. O. Stenflo (Kluwer, Dordrecht), 241
Stift, M. J. 2000, A Peculiar Newsletter, 33
Strasser, S., Landstreet, J. D., & Mathys, G. 2001, A&A, 378, 153
Traving, G., Baschek, B., & Holweger, H. 1966, Abh. Hamburger Sternwarte, Band VIII, 1
Vauclair, S., Hardorp, J., & Peterson, D. M. 1979, ApJ, 227, 526
Wade, G. A. 2000, in Magnetic Fields of Chemically Peculiar and Related Stars, ed. Yu. V. Glagolevskij, & I. I. Romanyuk, Special Astrophysical Observatory of Russian AS, 132
Wade, G. A., Bagnulo, S., Kochukhov, O. P., et al. 2001, A&A, 374, 265